URSI GASS 2021, Rome, Italy, 28 August - 4 September 2021

Numerical Analysis of Multifetal Exposure to Radiofrequency Electromagnetic Fields

Chen Zhang(1), Congsheng Li (1), and Tongning Wu* (1)
(1) China Academy of Industry and Communications Technology, Beijing, China, 100191, http://www.caict.ac.cn

Abstract

To numerically assess the multifetal exposure to radiofrequency fields (20 to 3600 MHz), one twin-fetal model was reconstructed and was merged to an adult female model to form the fetus-pregnant model. Numerical simulations using plane-wave revealed that the female adult was always significantly exposed compared to the fetuses for the surveyed frequency band. At lower frequencies, the twin fetuses were homogeneously exposed but the whole-body dosimetric difference could be as high as 270% at higher frequencies.

1 Introduction

The potential health risk of human exposure to radiofrequency (RF) electromagnetic field (EMF) has raised the public concerns on the specific age-groups [1]. Therefore, the assessment of child and fetal exposure to EMF becomes a topic of high interest.

As consequence, researchers published a serial of fetus-pregnant woman models [2-7] since 2000s. These models were reconstructed either from the medical images or by a hybrid approach using both the computer graphics and the realistic medical images. To our knowledge, the fetal models applied in these electromagnetic simulations were single fetus.

Multifetal pregnancy incidence was relatively low and it was about 33/1000 in 2016 in US [8]. However, it becomes much popular due to assisted reproductive technology. Up to date, there is no literature assessing the multifetal exposure to EMF due to the lack of the models. Therefore, it is necessary to investigate the dosimetric effect of the exposure for epidemiologic purposes.

2 Generation of the numerical models

One pregnant woman of 28 years old with 30 weeks of amenorrhea was involved in the MRI scan. The subject had monozygotic pregnancies. Fetal MRI was performed because of the high value (but in the normal range) of bilateral ventricles of one fetus.

A SIEMENS Avanto 1.5T scanner was used for data acquisition. Different sequences were applied:

- The fetal head was scanned by single-shot semi-Fourier imaging (HASTE sequence). Thickness was 4 mm without spacing, matrix 256 × 192, FOV 270 × 270.
- The fetal body was scanned with (1) TrueFISP sequence, thickness 4 mm scanning without spacing , matrix 256 × 192, FOV 297 × 390; and (2) T1 weighted gradient echo sequence (T1-FLASH sequence), thickness 5.5 mm without spacing, matrix 256 × 179, FOV 320 × 420.

The exemplary images are shown in Figure 1.

Figure 1. Abdominal MRI for the pregnant woman by coronal view. The fetuses close to the cervix were named by Fetus 1 (weighted 2 kg) and the fetuses far from the cervix were named by Fetus 2 (weighted 1.8 kg).

A relative lower intensity scanner (1.5 T) has been applied with thick slice interval in the imaging. The purpose was to limit the exposure and the scan time. However, the imaging quality was compromised. A semi-automatic segmentation on 2D slices and 3D volumes was performed. The original MR images were firstly corrected for bias fields and intensity non-uniformity using the N3 algorithm [9]. It was followed by image smoothing with an anisotropic filter. The selected methods included thresholding with different values, morphological operation (e.g., filling holes, opening and closing operators, etc.), region growing, and the graph cut method [10]. Manual segmentation and expert inspection were performed before head model reconstruction. Figure 2 shows the segmentation process. Various morphological methods have been used to keep the continuity of the contour.

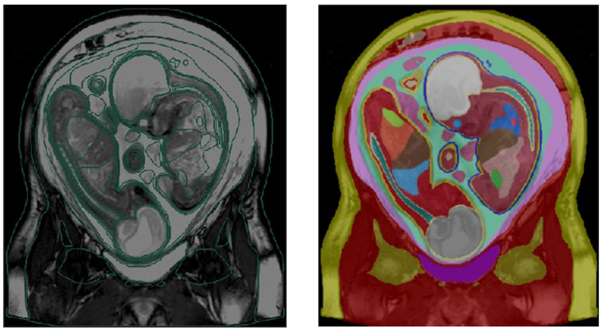

Figure 2. Segmentation for the uterus and the fetuses.

During MRI, the pregnant women were partially scanned. In order to generate a whole-body model, the Chinese female adult model was used [11]. We performed moving least square method to keep the continuity of the profile at the junction part.

The interactive segmentation tool, iSeg (ZMT, Zurich, Switzerland), and in-house software [12, 13] were used.

3 Simulations

This study aimed to investigate the dosimetric results of plane-wave exposure.

The FDTD method was used to calculate the E and H fields in the fetal models under RF EMF exposure. The FDTD spatial lattice was as 1 mm × 1 mm × 1 mm for 20 MHz to 3.6 GHz corresponding to a time update step as 1.8 ps. Sinusoidal E field was applied for the transverse mode (TEM) plane-wave exposure scenario and sinusoidal voltage source was applied for the localized exposure scenarios. Eight-layer perfectly matched layer (PML) was used as an absorption boundary condition. We inserted thirty grid cells between the PML boundary and the models. The number of time iterations varied from 2 periods (20 MHz) to 50 periods (3.6 GHz). Selection of the iterative time corresponded to a propagation distance of at least two times the maximum diameter of the computational domain.

Frequency-dependent dielectric parameters for the adult model were obtained from Gabriel et al [14]. The same values were applied for the fetuses.

The simulations were realized by SEMCAD-X v14.8 (SPEAG, Zurich, Switzerland).

Frequency-dependent whole-body averaged SAR (WBASAR) was calculated for the TEM plan-wave exposure scenario for human models. The E field polarization was parallel to the height of the anatomical model with propagation direction pointing to the face of the anatomical models. In the simulations, the model was isolated from the ground. WBASAR was normalized to the plane-wave power density as prescribed by the reference levels from the ICNIRP guidelines [15]. The simulation configurations are shown in Figure 3.

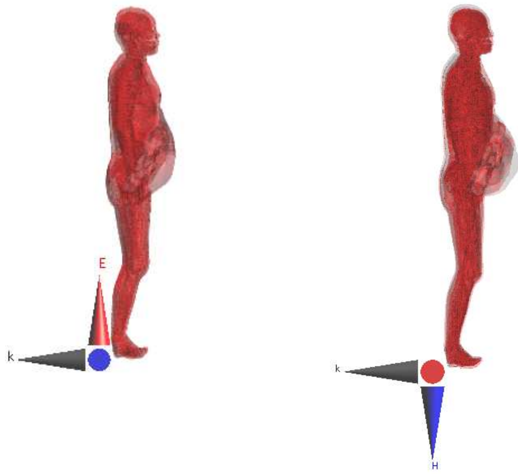

a b

Figure 3. Two incident configurations in the simulations. 3a is E-polarization parallel to body height and 3b is E-polarization parallel to body width.

4 Dosimetric Results and Discussions

WBSAR from two twin-fetus model is shown in Figure 4 for the incident configurations described in Figure 3a. Similarly, WBSAR from two twin-fetus model is shown in Figure 5 for the incident configurations described in Figure 3b.

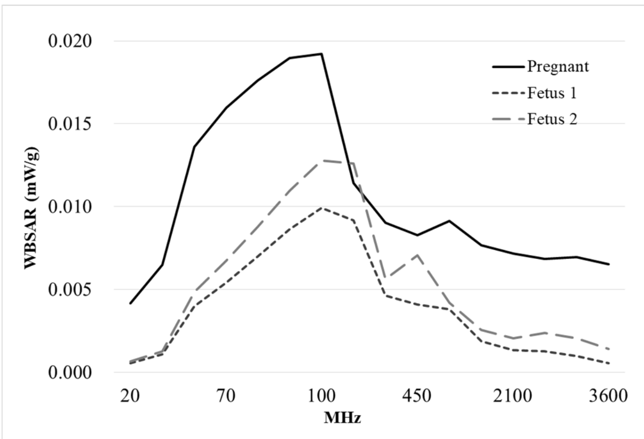

Figure 4. WBASAR for the scenario of E-polarization parallel to body height (Fig 3a). Fetus 1 is the individual close to cervix.

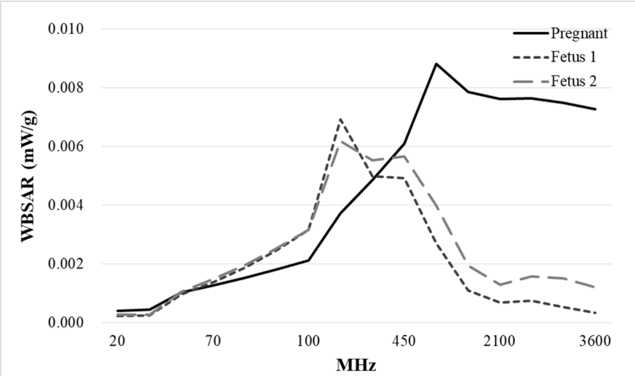

Figure 5. WBASAR for the scenario of E-polarization parallel to body width (Fig 3b). Fetus 1 is the individual close to cervix

The results indicated that the pregnant woman always had higher WBASAR for the E-polarization parallel to the adult height. The results were reasonable because a large portion of EMF power was absorbed by the skin, fat and amniotic fluid. The effect has also been found by the dosimetric study with single fetus. In contrast, the fetuses had higher WBASAR below 300 MHz for the case for E-polarization parallel to the adult width. It can attribute to the absorption resonant peak which occurred at around 150 MHz for the fetuses. In general, frontal incidence with E-polarization parallel to the adult height provided much higher RF absorption for both the adult and the fetuses.

At lower frequencies, the two fetuses had relatively slight difference in WBASAR whilst the deviation can be about 270% at 3600 MHz（Fig. 4）. It can be attribute to the skin depth. The wave penetrated effectively in the abdominal part of the pregnant woman so that the two fetuses absorbed similar amount of RF power. When the frequency increased and the wave attenuated rapidly along with the depth, the slight difference in relative positions of the two fetuses can cause sharp diverse power absorption. Fetus 1 which was close to the cervix had lower WBASAR, particularly at higher frequencies. It was because at the level of cervix, the distance between the adult skin and the fetus was large. The results indicated that we need to investigated the difference of power absorption due to the specific fetal positions, especially at higher frequencies.

5 Conclusions

One twin fetal model was reconstructed by semi-automatic segmentation of MRI images. The generated models were inserted to the abdominal part of the Chinese female model. By FDTD simulation using the TEM wave ranging from 20 – 3600 MHz, WBASAR was assessed by both the pregnant woman and the individual fetus. The results revealed that the pregnant adult was significantly exposed in comparison to the fetuses. The twins were comparatively homogeneously exposed at lower frequencies but the dosimetric deviation for them could be as high as 270% at 3600 MHz. The relative positions of the twin fetuses can also influence individual WBASAR.

6 Acknowledgements

The work is supported by the grants from National Natural Science Foundation of China (Grant No.61971445).

References

[1] R. J. Preston, “Children as a sensitive subpopulation for the risk assessment process,” *Toxicology and applied pharmacology*, 199, 2, September 2004, pp.132-141, doi:10.1016/j.taap.2003.12.030.

[2] P. Dimbylow, “Development of pregnant female, hybrid voxel-mathematical models and their application to the dosimetry of applied magnetic and electric fields at 50 Hz,” *Physics in Medicine and Biology*, 51, 10, April 2006, pp. 2383-2394, doi: 10.1088/0031-9155/51/10/003.

[3] X. G. Xu, V. Taranenko, J. Y. Zhang, and C. Y. Shi, “A boundary-representation method for designing whole-body radiation dosimetry models: pregnant females at the ends of three gestational periods—RPI-P3,-P6 and-P9,” *Physics in Medicine and Biology*, 52, 23, November 2007, pp.7023-7044, doi:10.1088/0031-9155/52/23/017.

[4] T. Nagaoka, K. Saito, M. Takahashi, K. Ito and S. Watanabe, “Estimating specific absorption rates in pregnant women by using models at 12-, 20 and 26-weeks’ gestation for plane wave exposures,” International Symposium on Electromagnetic Compatibility-EMC Europe. IEEE, 8-12 Septenber, 2008, pp. 1-4, doi: 10.1109/EMCEUROPE.2008.4786868

[5] J. Becker, M. Zankl, U. Fill and C. Hoeschen, “Katja-the 24th week of virtual pregnancy for dosimetric calculations,” *Polish Journal of Medical Physics And Engineering*, 14, 1, January 2008, pp. 13-20, doi: 10.2478/v10013-008-0002-4.

[6] L. Bibin, J. Anquez, J. P. de la Plata Alcalde, T. Boubekeur, E. D. Angelini, and I. Bloch, “Whole-body pregnant woman modeling by digital geometry processing with detailed uterofetal unit based on medical images,” *IEEE Transactions on Biomedical Engineering*, 57,10, June 2010, pp. 2346-2358, doi: 10.1109/TBME.2010.2053367.

[7] S. Dahdouh1, N. Varsier, A. Serrurier, J. P. De la Plata, J. Anquez, E. D. Angelini, J. Wiart and I. Bloch, “A comprehensive tool for image-based generation of fetus and pregnant women mesh models for numerical dosimetry studies,” *Physics in Medicine and Biology*, 59,16, July 2014, pp. 4583-4602, doi:10.1088/0031-9155/59/16/4583.

[8] G. Declercq and D. H. Z. Congress, “Birth by the numbers,” *National Vital Statistics Reports*, 67, 1 January 2018, pp. 1-55.

[9] J. G. Sled, A. P. Zijdenbos and A. C. Evans, “A

nonparametric method for automatic correction of intensity nonuniformity in MRI data," *IEEE Transactions on Medical Imaging*, 17, 1, February 1998, pp. 87-97, doi: 10.1109/42.668698.

[10] Y.Chen, Z.Wang, J.Hu, W. Zhao and Q. Wu, "The domain knowledge based graph-cut model for liver CT segmentation," *Biomedical Signal Processing and Control*, 7, 6, November 2012, pp. 591-598, doi:10.1016/j.bspc.2012.04.005.

[11] T. Wu, L. Tan, Q. Shao, C. Zhang, C. Zhao, Y. Li, E. Conil, A. Hadjem, J. Wiart, B. Lu, L. Xiao, N. Wang, Y. Xie and S. Zhang, "Chinese adult anatomical models and the application in evaluation of RF exposures," *Physics in Medicine and Biology*, *56*, 7, March 2011, pp. 2075-2089, doi: 10.1088/0031-9155/56/7/011.

[12] T. Wu, Q. Shao and L. Yang. "Simplified segmented human models for whole body and localised SAR evaluation of 20 MHz to 6 GHz electromagnetic field exposures," *Radiation protection dosimetry*, 153, 3, March 2012, pp. 266-272, doi: 10.1093/rpd/ncs105.

[13] C. Li, Z. Chen, L. Yang, B. Lv, J. Liu, N. Varsier, A. Hadjem, J. Wiart, Y. Xie, L. Ma and T. Wu, "Generation of infant anatomical models for evaluating electromagnetic field exposures," *Bioelectromagnetics*, 36, 1, 2015, pp.10-26, doi: 10.1002/bem.21868.

[14] S.Gabriel, R. W. Lau and C. Gabriel, "The dielectric properties of biological tissues: III. Parametric models for the dielectric spectrum of tissues," *Physics in Medicine and Biology*, 41, 11, April 1996, pp. 2271-2293, doi: 10.1088/0031-9155/41/11/003.

[15] A. Ahlbom, U. Bergqvist, J. H. Bernhardt, J. P. Cesarini, L. A. Court, M. Grandolfo, M. Hietanen, A. F. McKinlay, M. H. Repacholi, D. H. Sliney, J. A J Stolwijk, M. L. Swicord, L. D. Szabo, M. Taki, T. S. Tenforde, H. P. Jammet and R. Matthes, "Guidelines for limiting exposure to time-varying electric, magnetic, and electromagnetic fields (up to 300 GHz)," Health Physics, 74, 4, 1998, pp. 494-522.